5-2020

Multi Wall Carbon Nanotube (MWCNT) Laminar Composite Structures Reinforced with Titanium Carbide (TIC)

Rakibul Alam Shohan
The University of Texas Rio Grande Valley

MULTI WALL CARBON NANOTUBE (MWCNT) LAMINAR COMPOSITE STRUCTURES REINFORCED WITH TITANIUM CARBIDE (TiC)

A Thesis

by

RAKIBUL ALAM SHOHAN

Submitted to the Graduate College of
The University of Texas Rio Grande Valley
In partial fulfillment of the requirements for the degree of

MASTER OF SCIENCE

May 2020

Major Subject: Physics

MULTI WALL CARBON NANOTUBE (MWCNT) LAMINAR COMPOSITE STRUCTURES REINFORCED WITH TITANIUM CARBIDE (TiC)

A Thesis
by
RAKIBUL ALAM SHOHAN

COMMITTEE MEMBERS

Dr. Karen S. Martirosyan
Chair of Committee

Dr. Ahmed Touhami
Committee Member

Dr. HyeongJun Kim
Committee Member

May 2020

ABSTRACT

Shohan, Rakibul Alam, Multi Wall Carbon Nanotube (MWCNT) laminar composite structures reinforced with Titanium carbide (TiC). Master of Science (MS), May, 2020, 55 pp., 2 tables, 11 figures, 117 references.

Laminar composite structures based on twisted MWCNT yarn were crafted by integrating titanium and graphene at (80:20) wt. %, respectively, into multi wall carbon nanotube sheets. Titanium and graphene mixture addition has been used to enhance the mechanical properties of MWCNTs based composites structures through in situ formation of TiC by using combustion synthesis approach. Twisted yarn incorporated with powder mixture was heated up to 750 ^{0}C in Differential Scanning Calorimetry (DSC) to initiate the reaction among titanium, graphene, and MWCNTs. The characteristics X-ray peaks of the TiC phase were well observed on produced twisted yarns at 2θ =36, 39, 42, 62. We have also investigated MWCNT/TiC based composite morphology, TiC particles size and elemental atomic analysis by using the thermal field emission Scanning Electron Microscope (SEM) equipped with an Electron Dispersive X-ray Spectroscopy. It has been shown that the as-prepared laminar composites structures possess a tensile strength of 300 MPa which is worthy of comparison to the results available in literature.

DEDICATION

I dedicate my thesis to all healthcare workers who have been working on the frontline to curb spreading of COVID-19 pandemic in all over the world.

ACKNOWLEDGEMENTS

I would like to thank my supervisor Dr. Karen S. Martirosyan, a Professor in the Department of Physics & Astronomy at UTRGV for motivating and guiding me throughout the thesis. Special thanks due to Dr. Mkhitar Hobosyan, Ivan Davila, Dr. G.C. Dannangoda, and my fellow Ujjal Lamichhane for helping me to do different experiments.

TABLE OF CONTENTS

LIST OF TABLES

LIST OF FIGURES

CHAPTER I

INTRODUCTION

1.1 Background

Mankind is now experiencing its fifth and most intense industrial and technological revolution that broadly relies on composites structures and advanced composite materials. Scientists have been working on new techniques to replace expensive, heavy, short life and environment unfriendly materials with promising nano-architectured allotropes of carbons (Single Wall Carbon Nanotubes/ Multi Wall Carbon Nanotubes/ Graphene/ Graphite), which can take material science and engineering to the next level [1]. Moreover, composite fabrication maintaining a high degree of purity and uniform dispersity is crucial for structural applications. One- and two-dimensional nanomaterials like MWCNT and Graphene, respectively, as the composite filler materials have been investigated to fabricate many more advanced structural composites modified with optical, mechanical, electrical, and magnetic properties in recent advancement [2-5]. Reduced weight and high mechanical performance are the paramount features of these structural composites. Primarily, this is why our motivation is going to study high strength and lightweight laminar composite structures based on MWCNT twisted yarn reinforced with titanium carbides (TiC).

Laminar or yarn like composite structure have been widely used in weight-critical structures, such as aircraft, spacecraft, bullet-proof vests, radiation protection suits, spacesuits etc., owing to their high stiffness, strength, and thermal stability [6]. Recently developed high potential carbon structure, MWCNT yarn, has similar properties but far better mechanical properties compare to common carbon fibers [7]. Fundamentally, yarning is the way to increase the reliability and the durability of mechanical properties of MWCNTs composite structures, specifically Young's modulus and Tensile strength. To reduce the weight and complexity, the laminar composites can be employed towards outer space applications for the effective uses of solar sails and panels.

1.2 Structural and Composite Materials

Since the introduction of composite materials, physicists, chemists, engineers, and metallurgists have been working on laminar composites structure, ceramic matrix composites (CMC), metal matrix composites (MMC), natural fiber composites, and fiber reinforced polymers (FRP) composite structures etc. They have attracted more attention due to their high strength-to-weight ratio, high modulus-to-weight ratio, excellent fatigue resistance, good damage tolerance, excellent hardness, high thermal conductivity, exceptional mechanical strength, ductility at high temperature and virtue of making component of complicated shape [8]. Composite materials are being widely used for several decades in automobile, aerospace, rocket manufacture, transportation industries, civil infrastructure, sporting equipment as well as in medical and military application [9]. Due to their excellent and unique mechanical properties, composite materials have already been a powerful choice and a sustainable alternative to noble metals as well as to air-sensitive metal or oxide for structural applications in extreme environmental conditions.

Moreover, laminar composite structures have already offered a promising solution in the aircraft community by lowering manufacture-operation-maintenance cost and enhancing the performance of engaged materials and structures as well as becoming an attractive candidate for new generation aero-vehicles [10]. The use of laminar composite materials has been growing over time because these materials are the perfect choice for the structural applications that need low weight and high strength. Without exaggeration, we can safely say that the development of laminar structural composite materials has been playing an important role in modern technology, industry, and structural applications.

1.3 Multi Wall Carbon Nanotubes (MWCNTs)

MWCNTs have attracted a good attention for laminar composites structures due to its outstanding physical and mechanical properties possessed by individual CNTs, which outperform the properties of various advanced materials used for industrial applications. They are becoming an interesting material because of their unique one-dimensional structure, and their extraordinary electrical, thermal, and optical properties [11]. Other excellent attributes of MWCNTs comprise: a large aspect ratio, a low density, high thermal stability, chemical inertness, maintenance of mechanical properties at high temperatures and so on [12]. These exceptional characteristics have made CNTs a promising alternative to silicon, copper and aluminum in various fields [13] and more suitable for different novel applications in nano-mechanics, energy storage, biotechnology [14], catalyst support in fuel cells and reinforcement of materials [15]. Moreover, due to these characteristics, MWCNTs have been used in weaving into macroscopic objects like electrically conductive wire, bulletproof vests, materials which can absorb electromagnetic waves. They also being used as mechanical actuator [16] for artificial muscles, flexible batteries, sensor, and solar cells.

Harnessing these outstanding and intriguing properties of MWCNTs into application requires its existence on a macroscopic scale such as in the form of fiber or yarn in which CNTs are aligned to the fiber axis and parallel to each other [17]. The lightweight yarn-like structure made of MWCNTs fibers showed exceptional toughness, high surface area, resilience to bending stresses and good performance into structural applications [18]. MWCNT yarn and laminated sheets made from directly CVD or forest by spinning or drawing methods outperform carbon fiber for high-end uses, especially in weight critical applications having combined electrical and mechanical functionality.

However, synthesized CNT macrostructures such as yarn and sheets until now possess (or have) substantially lower mechanical, electrical and thermal properties than those of individual CNTs as the probability of a critical flaw scales up with volume. On the other hand, high surface area of CNTs can attenuate these inadequacies by introducing interfacial bonding (van der walls), and CNT yarns compare with carbon fibers can be knotted maintaining their strength [19]. Furthermore, forest-drawn CNT sheets coating with functional power has produced yarns which containing almost 95 wt. % powder. Organized CNT architectures such as vertically aligned forests, yarns, and sheet exhibit promise to enhance the properties of individual CNTs and opened up new functionalities comprising dry adhesion, large-stroke actuation, shape recovery, high damping, terahertz polarization, near -ideal black body absorption, and thermoacoustic sound emission [19-22].

Many researches have already been carried out to make the full use of CNT’s outstanding properties into applications in different ways. In this study, our intension is to exploit these unique properties of MWCNT as much as possible into application by fabricating macrostructural yarn like structure.

1.4 Integration of Titanium-Graphene mixture into MWCNTs sheets

In this study, we integrated titanium and graphene mixture into 30 MWCNT sheets stacked on top of each other to improve the mechanical properties of MWCNT twisted yarn through in situ formation of TiC. Graphene, a two-dimensional honeycomb sheet of sp2-hybridied carbon atoms, has significantly grown in interest in the fields of science, technology, and industry because of its exceptional properties, for instance, high thermal conductivity (~ 3000 w/mk), Young's modulus (~ 1.1 TPa), mechanical strength (~ 125 GPa) [23-25]. Also, graphene can be embedded in different modern industrials and electronics devices such as lithium-ion batteries, fuel cells, ultracapacitors, molecular sensors, transparent display, flexible electrodes, and transistors [26-30]. Physicists and materialists have been working on how to cultivate the outstanding properties of graphene. One possible route is to maximize the effective use of these properties into application by integrating them into composites. That's why we have used graphene nano flacks into our laminar composite structure to improve the mechanical properties. The incorporation of graphene into polymer matrices shows promising enhancement of mechanical properties [29]. Because of considerable difficulties in dispersion, fabrication, and their unrevealed interfacial chemical reaction, unlikely to graphene-polymer composites, the graphene metal composites were still little discussed. However, a number of recent advances in graphene-metal composites have been observed. For example, Hu and colleagues studied graphene reinforced titanium-based nanocomposites materials and found the nanoindentation hardness (almost 11 GPa) which was three times greater than the pure Ti, also the Young's modulus (200 GPa) was dramatically increased [32].

Titanium and its composites are being intensively utilized in marine, aerospace and military areas by virtue of their outstanding properties like high melting point, low density, high tensile strength at ambient temperature, excellent corrosion resistance, and great biodiversity, compare to steel and aluminum alloy [33]. But, because of their some significant drawbacks like wear resistance, low thermal conductivity, high cost and low mechanical strength at high temperature, many researchers propose carbon materials-Ti composites, such as carbon nanotubes-Ti and carbon fibers-Ti composites, to overcome the limitations [34,35]. Graphene, compared with carbon nanotube and carbon fibers, shows even more exceptional performance in thermal and mechanical properties. Adding a certain amount of graphene, the thermal and mechanical properties of pure Ti and its alloys may be effectively increased. Ti-Gr nanocomposites synthesized by laser sintering showed more than two times Vickers Hardness value of titanium [36]. These all characteristics of Ti composites specially with graphene substantially signify the reasons behind incorporating the Ti/Gr into MWCNT structure to enhance the mechanical properties. The intention of this research is to explore the experimental aspects of Ti/Graphene/MWCNT composites structures because a handful of interdisciplinary studies of Ti/Graphene composites have been done so far and mostly rely only on functional and theoretical calculations [37,38].

1.5 In situ formation of TiC inside MWCNT yarn

Titanium carbides have attracted a great deal of attention because of their high chemical resistance, high heat resistance, short bonds, good corrosion resistance, low weight, biocompatibility, exceptional mechanical strength, chemical stability, high elastic modulus, high wear resistance, low heat-conductivity coefficient and good electrical conductivity for many structural applications. They are being used for metal working tools, high temperature heat exchanger, turbine engine seals, grinding wheels, magnetic recording heads, bullet proof vests, and carbide steel, etc [39,40]. It has received considerable commercial interest as well [41]. The purpose of this study is to synthesize TiC inside MWCNT yarn so that it can reinforce the mechanical properties of as produced MWCNT twisted composite structure.

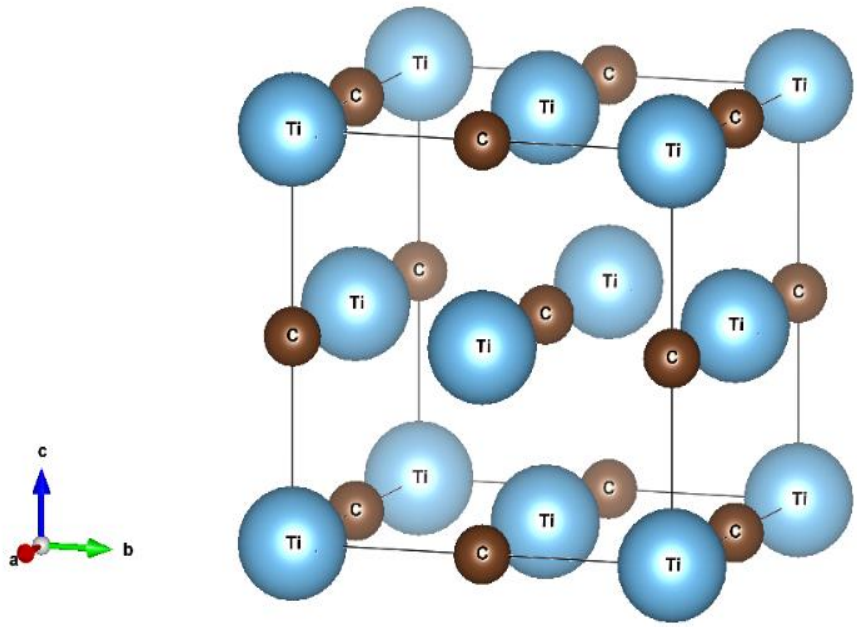

Figure 1: FCC structural configuration of TiC. (Drawn by ChemDraw software)

TiC has been used as a reinforcement for the metal matrix composites (MMC) by virtue of its excellent properties, such as high melting temperature (3250^0 C), low density (4.93 g/cm^3), high hardness (2895-3200 HV), high chemical stability and high elastic modulus (Young's modulus of 410-510 GPa) [42], good wettability and strong interfacial bonding with the metal matrix. Publications in the literature proves that TiC reinforced metal composites shows good wear resistance and higher mechanical properties [43-46]. TiC produced by mechanical alloying have outstanding resistance to oxidation and corrosion because of homogeneous distribution and adhesion between particles and being attractive composite materials in aerospace application [47,48. Excellent compatibility between TiC grain and stainless steel makes the TiC grains the suitable reinforcement agent for the stainless steel. The formation of TiC layers inside the Cu-CNT nanocomposites substantially improves the interfacial bond between the CNTs and the copper matrix [49]. The articles [50,52] verified the practical roles of carbides by establishing the thermal conductivity of Cu-Ti-CNTs that is sufficiently higher than the Cu-CNTs. It was disclosed that the tribological properties of the nanocomposites has been significantly enhanced with greater quality TiC, which is resulted by using the CNT and graphene as carbon sources. In comparison to using graphite as a carbon source, graphene and CNT lowers 49% and 15% in wear volume loss and decrease 6% and 16% in friction coefficient successively [52]. Hard TiC particles are being used to improve the wear resistance and harness of the Cu matrix composites as investigated by Yang et al. [51]. About ten-fold strength improvement has been noticed in titanium matrix composites (TMC) by reinforcing with TiC [54,55].

1.6 SHS methods of amalgamation

Many synthesis processes were studied and proposed to produce TiC such as chemical vapor deposition (CVD) [56], thermal plasma synthesis [57], carbothermal reduction process [58], reactive hot pressing (RHP), spark plasma sintering (SPS) [59,60]. self-propagating high temperature synthesis (SHS) or combustion synthesis [61 - 63], mechanical alloying [64], microwave sintering [65], reactive hot pressing, exothermic dispersion, direct melt oxidation, flux-assisted synthesis and so on. Synthesizing TiC by a direct reaction between Ti and carbon under vacuum at high temperature is expensive because it requires high energy. As well as the thermal plasma synthesis and the chemical vapor deposition have very high operating cost, and the sintering process consumes large amount of energy. Even though the TiC mixture prepared by high energy ball milling can significantly reduce the ignition temperature [66], fabrication process is convoluted and need further modification for industrial purpose. Among all of them, on the other hand, the prominent, cost effective, and low energy consumption SHS process, by using large quantity of heat of reaction, has got more attention [67,68]. Martirosyan's research group at the University of Texas Rio Grande Valley successfully published several reports based on combustion synthesis [69-74] including experimental [77-77] and theoretical [78-80] investigations.

Self-propagating high temperature synthesis (SHS) process, which also referred to as combustion synthesis or highly exothermic process, is a kind of self-sustaining synthesis technique in which precursor is triggered at one end by external high energy input (e.g. laser beam, heated coil) to initiate the reaction and once ignited, the highly exothermic reaction between constituents or between constituents and compounds turns into self-sustaining and converts progressively the constituents into product by no means of any external energy [69-74]. This synthesis technique has already been an attractive method for researchers to produce composite or refractory materials. K.S. Martirosyan and A.S. Mukasyan [82] explained all about combustion synthesis of nanomaterials explicitly and precisely in their book. By using this convenient method, a large scale of different materials like nitrides [83], borides [84] intermetallics [85], carbides [86], silicides, carbonitrides, composites, hydrides, chalcogenides, complex oxides, have been fabricated. The compelling advantages of this technique comprise: i) high purity and refined microstructure of product, ii) energy and time efficient, iii) simplicity of process and equipment, iv) high reaction rate, v) simultaneous formation and densification of product, vi) substituting the raw materials with cheaper one, and most importantly, vii) low production cost [87]. By applying the SHS method, many organic compounds and materials, more than 700, have been synthesized. This method is not only suitable for solid-solid system, but also for solid-liquid and solid-gas combustion system. Porous TiC from titanium and carbon powder were produced by the SHS process, proposed in [88]. Also, by this process, Holt and Munir [89] and Yamada et al. [90]

effectively synthesized dense TiC composites from titanium and carbon powders. The self-sustaining exothermic reaction in the SHS process can provide high temperature required for inorganic compounds, more than 2000 K, and for intermettalics, more than 1000 K. Finally, we have chosen the SHS process because it's various merits over conventional methods to produce in situ TiC inside MWCNT twisted yarn. Most importantly, highly exothermic reaction being ignited between constituent powder requires comparatively low temperature below 1000 ^{0}C in the SHS process.

1.7 Literature reviews

In literatures, many researchers have been conducting research to improve the mechanical properties of MWCNT composite yarn. To the best of our knowledge, no comprehensive reports have been published yet about the mechanical properties of MWCNT laminar composite structures reinforced with TiC in any other literature. Our synthesized laminar composite structures exhibit the tensile strength of 320 MPa which is not the best but comparable to the results available in literature. CNT yarn produced through Chemical Vapor Infiltration (CVI) shows increased tensile strength from 61 MPa for the pristine yarn to 159 MPa for 2 hours CVI served yarn. The excellent increment of stiffness also has been noticed in CVI yarn treated for 2 hours which is from 1.68 GPa for pristine yarn to 11 GPa for as-synthesized yarn [91]. Tensile strength of 5-ply yarn composite with ratio of epoxy: modifier: hardener (60:40:20) and 25- ply yarn composite (100:0:25) are reported as 319.8 MPa and 261.4 Mpa, respectively [92].

Composites made from bamboo-type carbon nanotubes shows tensile strength of 170 MPa and Young modulus of 4.7 GPa comparing with 120 MPa and 2.3 GPa in composites synthesized from common hollow MWCNTs [93]. The strength of the CNT/nylon 6,6 composite were improved to 320, 540 and 630 MPa with stretch rations of 2%, 5% and 7%, respectively [94]. Another practical way to improve the mechanical properties of MWCNT yarns structures through polymer dip coating [95]. Zhang et al. revealed considerable improvement of tensile strength of the CNT yarn by infiltrating with a polymer [96]. Increment of load capacity of CNT yarn by post spun twisting has been reported by Zhu et al [97].

It has also been reported in literature that molecular functionalization and electron-beam irradiation both were consider as a technique to increase the tensile strength and Young modulus of the bulk CNT yarn composites by 25% and 88%, respectively [98]. Kai Liu et al. synthesized CNT/ polyvinyl alcohol (PVA) yarns having tensile strength up to 2 GPa and Elastic modulus more than 120 GPa, much higher than the twisting (1 GPa) and simply twisting (0.5 GPa) yarn [99].

Researchers have been working on yarn like laminar composite structures to improve the mechanical properties of MWCNTs in different ways. However, usually pristine MWCNT yarns lack required stability under load. In this study, we have introduced a method for stabilizing MWCNT yarn using highly exothermic reaction to produce and deposit TiC into yarn. In situ produced TiC effectively binds adjacent MWCNT to restrain inter-nanotubes sliding effect load, which therefore increase the durability of MWCNT yarn structure. Neighboring nanotubes slide each other under load in yarn, which causes a high extents of stress relaxation and permanent elongation. As a result, mechanical properties i.e. tensile strength and young's modulus of yarn also changes with load, which is not acceptable for most structural application. Therefore, it is crucial to stabilize and sustain the MWCNT yarns.

1.8 Objectives

a) Synthesis of composite or yarn like structure based on Multi Wall Carbon Nanotubes (MWCNTs) twisted yarn.

b) Reinforcement of this laminar composite structures by in situ production of TiC inside yarn.

c) Thermogravimetric analysis of this structure composites.

d) Morphological analysis of our as produced yarn like structures.

e) Investigating the mechanical properties of as synthesized laminar composite structures.

1.9 Hypothesis

Addition of titanium and graphene mixture inside the MWCNTs sheets may increase the mechanical properties of as synthesized MWCNT laminar composite structure by in situ formation of TiC.

1.10 Layout of the thesis

- Chapter 2, a detail description of general properties and applications of Titanium, Carbon Nanotubes, and Graphene are presented.
- Chapter 3, we discussed the methods of preparing our sample and laminar composite structures.
- Chapter 4, results are analyzed and discussed.
- Chapter 5, this report is concluded with some remarks on the results.

CHAPTER II

PROPERTIES OF MATTERS

We have used titanium, MWCNT, and graphene in this study because of their outstanding characteristics which is important for structural applications. They have extraordinary mechanical properties, thermal properties and most importantly they are compatible with the environment.

2.1 Titanium

Chemical element, Ti, atomic number 22 and atomic weight 47.90, is a silvery gray transition metal. As Titanium belongs to the first transition group, chemically its behavior shows many similarities with silica, chromium, zirconium, and vanadium. It is a strong, corrosion-resistant, lustrous metal. Titanium of this size (149 μm) is not pyrophoric, and is covered by few nano (4-5 nm) layer of oxide. English mineralogist and chemist William Gregor discovered a compound of titanium and oxygen for the first time in 1791 and separately rediscovered in 1795, and finally named by the German chemist Matrin Heinrich Klaproth.

2.1.1 Properties

It is high-strength, lightweight, low-corrosion structural metal. It is 60% heavier than aluminum and 45 % lighter than steel.

- Electron configuration: [Ar] $3d^1$ $4s^2$
- Density: 4.506 g/cm^3 at 25^o C
- Melting point: 1670 ^{o}C
- Boiling point: 3287 ^{o}C
- Specific heat capacity: 524 $JKg^{-1}K^{-1}$
- Young's modulus: 115.7/107 GPa
- Shear modulus: 43.8/38 GPa

2.1.2 Applications

It also works as an excellent alloying agent with many metals like aluminium, iron, molybdenum. These alloys have been used for many high temperature structural applications due to extremely high melting temperature, excellent hardness, high thermal conductivity, exceptional mechanical strength, and great chemical resistance. Also, they have attracted a good attention for aircraft and spacecraft application [33-35].

Titanium is being used in orthopedic implant devices because of its outstanding high strength, rigidity, and their genuine mechanical performance. Prosthetic hip and knee replacement, bone-plates and screws, pace-makers, and cranial plates of skull fractures are prime examples of titanium implants used in orthopedics [100]. Titanium dioxide (TiO_2) has opacity to UV light damage and auto cleaning capacity leading their uses as a white pigment in outside painting [101]

2.2 Carbon Nanotubes (CNTs)

CNT sparked the imagination of different research groups and organization around the world. It is an one dimensional beehive-shaped nanostructural tube with sp2 hybridized carbon atoms. In 1952, Radushkevish and Lukyanovich first investigated and explained CNTs, and later on, Oberin observed SWCNTs in 1976. In recent history, the discovery of CNTs is attributed to Iijima, who described multi-walled carbon nanotubes for the first time during C60 molecule fabrication. Since their discovery by Iijima in 1991, carbon nanotubes have fascinated researchers with their possibilities for different commercial applications.

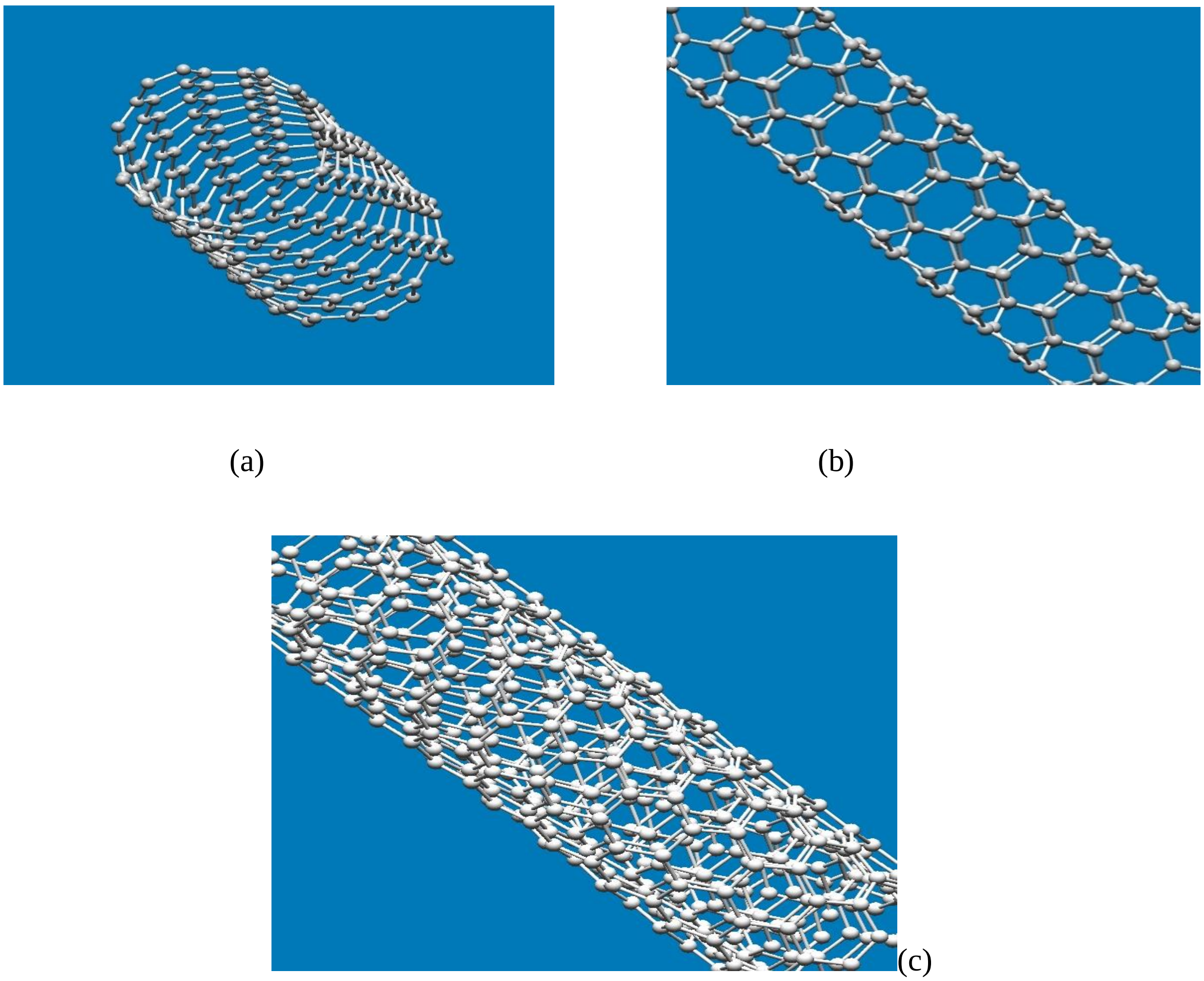

(a) (b) (c)

Figure 2: Zig-zag (a), SWCNT(b) and MWCNT (c) (Drawn by Nanotube modeler software)

2.2.1 Properties

Carbon nanotubes are known as nano-architectured allotropes of carbon, composed of layer of graphene sheets that are wrapped having a cylindrical shape. Approximate thickness of CNTs is 1/50000th of human hair. They usually exist in three different geometries: a) armchair, b) zig-zag, and c) chiral. CNTs can be either metals or narrow-band semiconductor based on the ways of rolling of graphene sheets. Over the years, researchers are working to understand the intriguing properties of CNTs. They exhibit some outstanding properties like a large length-to-diameter ration, a high degree of stiffness, exceptional resilience. By controlling the diameter, wall nature, chirality, and length of CNTs, these properties of CNTs can be manipulated.

Two types of carbon nanotubes that can have high structural perfection. Single walled carbon nanotubes (SWCNTs) consist of a layer of graphene sheet folded into a cylindrical tube. Multiwall carbon nanotubes (MWCNTs) are composed of several layers of graphene sheets like rings of a tree trunk. Depending on the direction of graphene sheet rolled to form a nanotube cylinder, CNTs can be either metallic or semiconducting. CNTs have a diameter approximately from 0.4 nm to more than 3nm and length can extend up to millions of times of the diameter. The interlayer space in MWCNTs is around 3.4 Å, which is similar to space between graphene sheets interlayer. MWCNTs have diameter ranges from 1.4 to 100 nm.[20,21]. Small-diameter SWNTs have a high Young's modulus and high tensile strength. Properties for the nanotubes can be tuned by tailoring the diameter.

Table 1: Comparison between MWCNTs and SWCNTs

MWCNT	SWCNT
Several graphene layers	Single graphene layer
Easy bulk synthesis	Difficult bulk synthesis
High purity	Poor purity
Structure is complicated	Easy assessment and characterization
Not easily twisted	Twisting is easy
Aggregation in the body is high	Aggregation in the body is less
Lesser chances of defects during functionalization	Greater defects chances during functionalization

2.2.2 Applications

CNTs have outstanding mechanical, chemical, thermal, electrical, and optical properties [102,103]. The thermal conductivity of CNTs is more than double of diamond which was the best-known thermal conductor before that CNTs identifications. The sp^2 carbon-carbon bonding inside CNTs has made them remarkably mechanically strong [104]. The nanotubes are considered extraordinary for the variety of structural applications because of high mechanical strength with a Young's modulus value of 1000 GPa which is about five times higher than steel [105]. The tensile strength of CNTs is approximately 63 GPa which is almost 50 times greater than steel [106]. Nanotubes also have been widely used in fabrication of nanoscale electronics devices.

With the growing demands in energy sector, researchers are relentlessly investigating all the existing resources of energy. They also studied all the promising substitutes whether renewable or non-renewable. Solar energy as a cost effective, abundant, and sustainable source of energy, could be a promising solution for sustainable production and the storage of electrical energy for different applications, such as transport, portable devices etc [107,108]. To overcome the limitations of solar collector, which is low efficiency of thermal conversion, Carbon nanotubes attracted a great attention because of their excellent performance as a solar absorber and hear transfer fluid. Stable CNT fluid, which is a result of modified MWCNTs by beta cyclodextrin, enhances the thermal conductivity and solar absorptivity.

CNTs, which is considered as p-type semiconductor, based photovoltaic cells (PVCs) have already attracted an intensive attention in renewable energy sector [109]. The amalgamation of CNTs with electron donors exhibits a promising idea to exploit the solar energy and transform this energy into electrical energy [110]. Carbon-on Si is a sustainable design to produce solar cells with excellent conversion effectiveness [111].

Ultracapacitors, which are devices for energy storage, with electrodes composed of CNTs have exceptional power density about fourfold higher than batteries, an energy density of almost 60W/Kg, and a lifespan more than 300,000 cycles [112]. This considerable improvement in the DLC power density attributed to the extraordinary conductivity and surface area gained form CNTs.

As an electrode material for batteries, CNTs have already been considered a promising candidate due to their remarkable electrochemical properties. For the technologically recognized lithium ion batteries (LIBs), outstanding anode materials come from the synthesis of SnO-CNT composites. The combination of CNTs with Si nanoparticles shows a new idea to fabricate high-performance electrode for LIBs. Recently CNTs have been using in microbial fuel cells because of their unique and excellent intrinsic properties like good electrochemical stability, corrosion resistance, and high conductivity [113,114].

CNTs have high surface area to volume ration and an organized distribution of pore size as compared to activated carbon. For these characteristics, they have excellent sorption ability. Clean water is crucial for all living organism to nourish their life [115]. CNTs as adsorbents can remove various heavy metals from water and can be widely used for water treatment applications. CNTs based ultrasensitive sensors are being applied to detect mercury which is very toxic to all living organisms [115]. In addition to the removal of toxic metals, CNTs are contributing to wipe various organic pollutants in water treatment process. They are also considered as an outstanding absorbent for the treatment of organic dyes owing to their large surface area and extraordinary properties. Emulsified oil in water, which have very negative impact on the living organism and environment, have been remove by ANTs. The most prominent application of functionalized CNT-based nanobiosensors is to detect the DNA sequences in our body [116]. As well as CNT- based pressure sensors are being used in kidney dialysis machines, eye surgeries, respiratory devices, and hospital beds.

2.3 Graphene

Graphene, or mono-layer graphite, is a single-atom-thick and two-dimensional honeycomb sheet consisting of sp2-hybridied carbon atoms which are tightly packed in a hexagonal crystalline structure (Park & Ruoff 2009). It is the building block of all graphitic carbons. However, graphene shows magnificent properties than its mother material which is graphite. Due to its tightly packed carbon atoms and sp2 hybridization, graphenes are more stable.

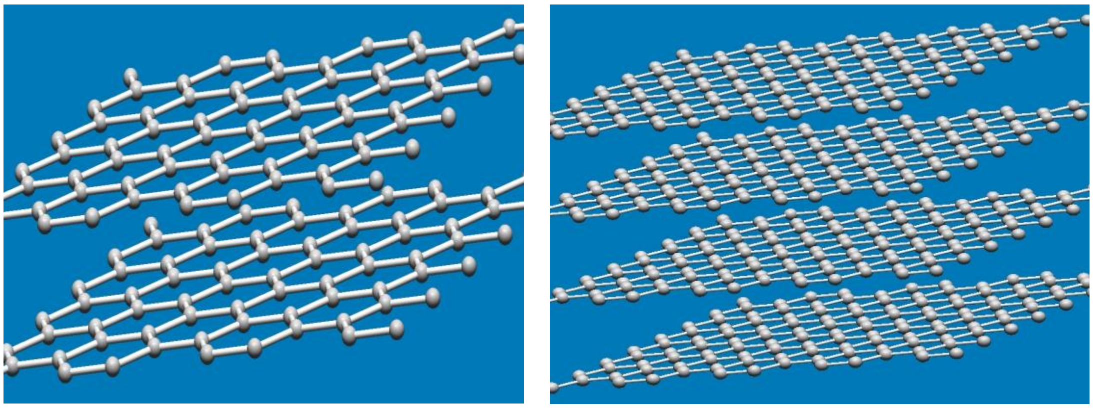

(a) (b)

Figure 3: Two layered graphene sheets (a) and Four layered graphene sheets (b). (Drawn by Nanotube modeler software)

In 2004, pioneer researchers Geim and Novoseloy conducted an outstanding research in the University of Menchester leading to isolation of a single sheet of graphene using scotch tape method on a silicon wafer [117]. Since the discovery of graphene, many researchers have been conducting research on it in the scientific community. Furthermore, due to its outstanding optical, electronic, thermal, and mechanical properties, it has been utilized in several industrial applications.

2.3.1 Properties

Among two dimensional crystalline layered materials, graphene has arguably the largest surface area to volume ratio. Also, it has highest ratio of edge atoms among any allotropes of carbon which make the graphene more chemically reactive. Since it possesses high aspect ratio (length many times larger than that of their width) which is tremendously useful parameter for enhancing mechanical and electrical properties of composite structure. Atom-thick layer of ring-bound carbon atoms being spread in graphene sheets are exposed to its surface. This excellent characteristic gives graphene an array of distinctive surface chemical, physical and electronics properties, which persistently opening doors for new applications in condensed matter physics and nanotechnology. Remarkable low-energy electronic structure of single-layer graphene can absorb white light by ~ 2.3 %.

- Strength: monolayer, defect free graphene is the strongest material tested to date with a strength of 42 N/m, which is equivalent to 130 GPa. It is more than 200 times stronger than steel.
- Elasticity: it can be stretched up to 20%, whereas steel can be stretched only 1%.
- Young's modulus: ~ 1TPa.
- Electron mobility: highest carrier mobility of 200,000 cm^2/Vs at room temperature which is more than 100 times higher than silicon.
- Thermal conductivity: ~5000 W/mK which is more than 100 times greater than copper.
- Current density: more than 10^8 A/cm which is around 100 times larger than copper.
- Optical absorption coefficient: 2.3 % which is around 50 times higher than Gallium arsenide (GaAs).
- Surface area: it has highest surface area of 2630 m^2/g meaning less than 3 grams of graphene could cover a soccer field.
- Impermeability: it can block even the smallest atom (Helium).

- Electrical resistivity: 10^{-8} Ω which is around 35%less than copper.
- Atomic thickness: 0.335 nanometers.

2.3.2 Applications

Graphene can detect changes in its surroundings at micrometer scale and individual events on a molecular level providing a high degree of sensitivity. Its outstanding properties are beneficial in sensor applications like biosensor, DNA sensors and gas sensors etc.

To increase the efficiency and improve the charge/discharge rate of the battery, graphene has already been integrated into both the anode or the cathode in different battery system, such as lithium-ion batteries, lithium-sulphur batteries and so on. Since it exhibits a high aspect ratio and dangling bonds at both sides of the sheet, graphene can be a perfect ingredient for use in electron emission display.

Graphene is being incorporated into many materials to increase the strength and make it lightweight which is very crucial for aviation industry. This composite material could save lots of fuel consumption and money.

CHAPTER III

METHODOLOGY

Our approach of methodology involves producing titanium and graphene mixture by using ball-miller first, and then synthesizing laminar composite structural yarn by incorporating titanium/graphene mixtures inside MWCNTs sheet.

3.1 Titanium and Graphene mixture preparation

Raw materials were commercial titanium powders (149 µm in size, 99.9% purity, Sigma-Aldrich) and graphene nanoflakes (12 nm in size, 99% purity, Sigma-Aldrich). The mixture was prepared with titanium and graphene powders according to the stoichiometry derived from the expected reaction equation: Ti + C = TiC, which is (80:20) wt. %. The mixed powders were placed into ceramic cylindrical container of ball-miller with 30 ml of isopropanol as milling media and the weight ratio between powder mixture and balls was 20:1. We used MSK-SFM-3 high speed vibrating ball miller at a speed of 1200 rpm (revolutions per minute)/ 20 Hz for 8 minutes with the period of 40 sec to mechanically activate the mixture particles and to produce homogeneous mixture samples. The wetted mixture sample from the ball-miller was heated in an oven for 30 minutes to evaporate the isopropanol and then titanium/graphene dried mixture samples were obtained.

3.2 MWCNT twisted yarn preparation

We used commercially synthesized vertically aligned CNT forests grown on silicon wafers by chemical vapor deposition (CVD) to produce well aligned MWCNT sheets. The synthesized forest has height up to 280 µm and single carbon nanotubes with an outer diameter of ~20 nm. As well as the volumetric forest density of synthesized CNT arrays was 63.8 mg/cm3. The aligned MWCNT sheets were drawn from the side of the synthesized CNT forests using a razor blade and a short-pointed piece of wood like toothpick by hand. 30 layers of MWCNT sheets were extracted and stacked on top of each other. This stacked MWCNT sheets has width of 2 cm and was placed between two rods separated by a distance of 7 cm. The weight of stacked 30 MWCNT sheets was measured as ~1 mg. Forest-drawn MWCNT sheets were overlaid with titanium and graphene materials by dispersing their mixture solution using small paint brush. The coating solution was prepared by mixing titanium and graphene powder in isopropanol and sonicated for 20 minutes to get homogeneous solution. The laminar composite yarn was prepared by twisting 30 layers of MWCNT/titanium/graphene sheets with width and length of 0.123 mm and 7 cm, respectively.

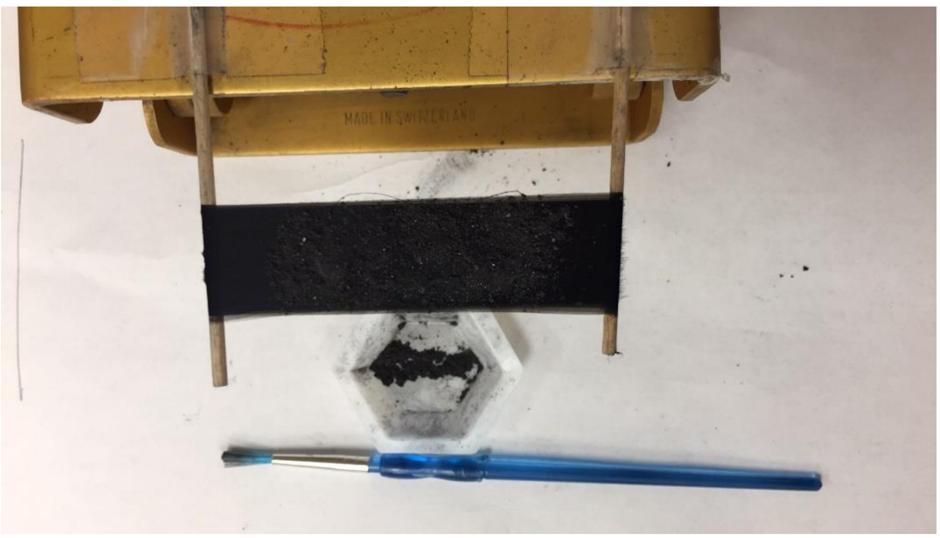

Figure 4: Integrating titanium/graphene mixture powder into MWCNT sheets.

CHAPTER IV

RESULTS AND DISCUSSION

4.1 Differential Scanning Calorimetry (DSC) analysis

The DTA/TG curves of Ti/Graphene mixture powder at 20 ^oC/min heating rate under argon flow of 100 ml/min are presented in Figure 5.

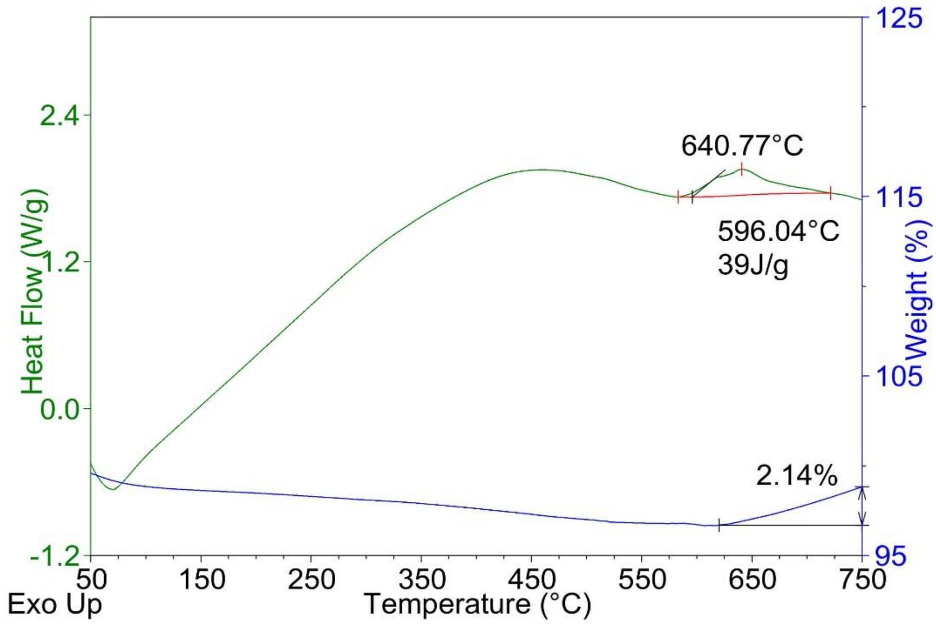

Figure 5: DTA-TG curves for the titanium and graphene mixture powder at heating rate 20 ^oC/min under argon atmosphere.

In Figure 5, green curve represents the Differential thermal analysis (DTA) of Titanium/Graphene mixture at heating rate 20 ^{o}C/min under inert atmosphere. This inert atmosphere has been created by flowing argon gas into the chamber in order to prevent Ti/Graphene mixture from being oxidized with atmospheric oxygen. At the very beginning of this DTA curve, one endothermic trough has been observed below 100 ^{o}C due to loss of absorbed moistures which can be present in the titanium and graphene mixture from the surroundings. Then the system is being started heating up to reach the activation energy which is required to initiate the chemisorption reaction between adsorbent (Titanium) and adsorbate (Graphene). This reaction involves covalent bonds usually in sticking the adsorbate to the adsorbent and is considered as an exothermic reaction. As it's clearly seen from DTA curve (green line) that the ignition starts at 596 ^{o}C and an exothermic reaction has been taking place at 641 ^{o}C. The heat released by the exothermic reaction between titanium and graphene is 39 J/g which raises the temperature of the sample mixture to such a level that the reaction becomes self-sustaining.

The blue curve represents the Thermogravimetric analysis (TGA) of Titanium/Graphene mixture. As we can see from figure 5, all over the interval of temperature increasing, TG signal is virtually constant. Only 2% of weight gain has been observed on this TG curve around 630 ^{o} C which is insignificant amount corresponding to primary weight (15mg) of the sample mixture. The reason for this small amount of weight gain could be forming TiO2 by oxidizing with the oxygen which may present in Ti/Graphene mixture. Another reason could be using argon gas which was not 100% pure.

The DTA/TG curves of titanium/graphene mixture dispersed into MWCNT twisted yarn at 20 ^{o}C/min heating rate under argon flow of 100 ml/min are presented in Figure 6.

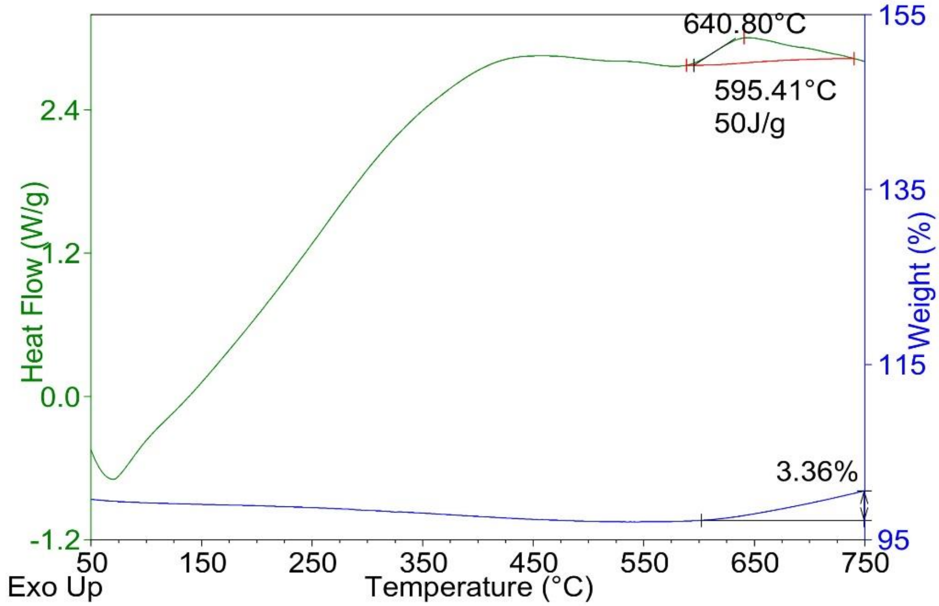

Figure 6: DTA-TG curves for the Titanium/ Graphene mixture integrated into multiwall carbon nanotube (MWCNT) twisted yarn at heating rate 20 ^{o}C/min under argon atmosphere.

In figure 6, green curve represents the Differential thermal analysis (DTA) of Titanium/Graphene mixture embedded multiwall carbon nanotube yarn. Inert atmosphere has been created by flowing argon gas into the chamber in order to prevent Ti/Graphene mixture integrated twisted yarn from being oxidized with atmospheric oxygen. Endothermic trough below 100 ^{o}C is due to loss of absorbed moisture that can be present while dispersing titanium and graphene mixture into MWCNT sheets from the surroundings. Then the system is being heated up to reach the activation energy which is required to initiate the chemisorption reaction between adsorbent (Titanium) and adsorbate (Graphene, MWCNT). This reaction involves covalent bonds usually in sticking the adsorbate to the adsorbent and is considered as an exothermic reaction. As it is seen form the DTA curve that the ignition starts at 595 ^{o}C and an exothermic reaction has been occurred at 640 ^{o}C. The heat released by the exothermic reaction among titanium, graphene, and MWCNT is 50 J/g which raises the temperature of the sample to such a level that the reaction becomes self-sustaining. The heat released from this exothermic reaction is higher than that the heat released from the Ti/Gr mixture only. One can assume that the more energetic reaction has been occurred inside MWCNT twisted yarn due to presence of more absorbate (carbon source). We can assume that the reaction takes place among titanium, graphene and CNT, and heat can remove the internal stress from MWCNT yarn and toughen it. The blue curve represents the Thermogravimetric analysis (TGA) of MWCNT yarn. Only 3.3 % weight gain has been observed on this curve around 600 ^{o}C which is negligible amount. The reason for this trace amount of weight gain could be forming TiO2 by oxidizing with the oxygen which may present in MWCNT/ Graphene interlayers. Another reason could be using argon gas which was not 100% pure.

Effective ignition of titanium is difficult because of oxide layer forming naturally on the surface of titanium. We used nano sized graphene flakes which is considered as one to few layers of graphene and generate high temperature which allows increasing the amount of TiC. Graphene has a high specific surface area of 1168 m^2/g and burning starts around 350- 500 ^{o}C due to large interlayer spacing of graphene sheets (5.1 Å). This spacious interlayer is mostly because of graphene curvature. Graphene shows reactive due to the high accessibility and active site over a large surface area. Thus, the high specific surface area of this graphene sample ensures the availability of carbon atoms on the surface.

4.2 X-ray Diffraction (XRD) analysis

The XRD patterns of synthesized TiC to reinforce MWCNT yarn by high energy exothermic process are shown in Figure 7.

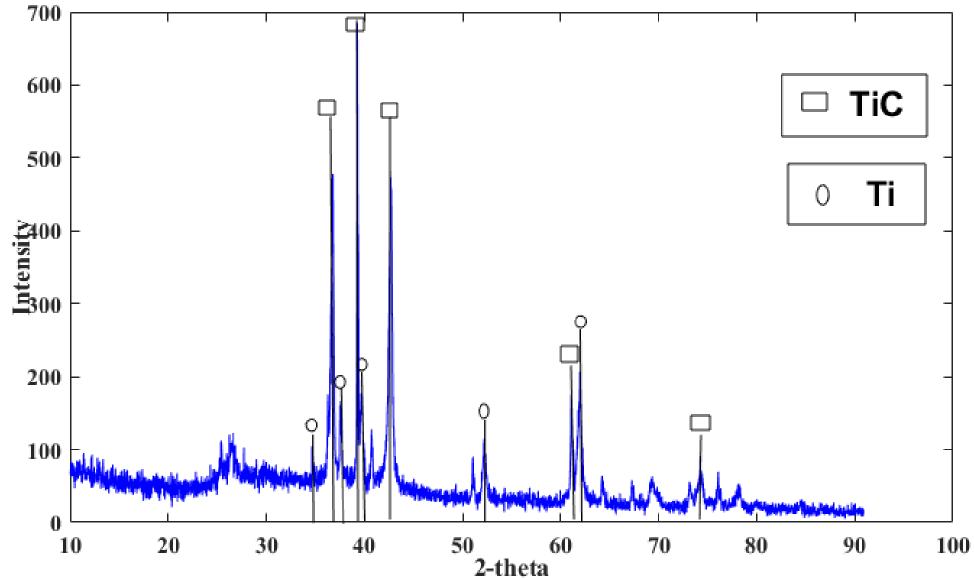

Figure 7: XRD spectra of TiC and unreacted Ti particles in Ti/Graphene mixture after combustion in DSC.

In Figure 7, as we can clearly see form the X-ray diffraction graph that only two prominent phases, Ti and TiC are clearly observed at their appropriate theoretical angular positions, meaning nearly full conversion of Ti and Graphene mixture into TiC in XRD level. Based on the intensity of characteristics peaks, the strongest XRD peaks signifies the TiC phase at 2-Theta= 36, 39, 42, 62 suggesting that the synthesized TiC possess high purity and well crystalline. It is also noticeable from figure 7 that small amount of Ti particles remain unreacted in the mixture and their phase was identified at 2-theta= 35, 37, 40, 52, 62. One possible reason for this unreacted Ti particles could be high concentration of Ti present in Ti/Graphene mixture. It can be assumed form this XRD analysis that TiC is the final thermodynamically stable phase of the Ti and Graphene system in this combustion synthesis.

4.3 Scanning Electron Microscope (SEM) analysis

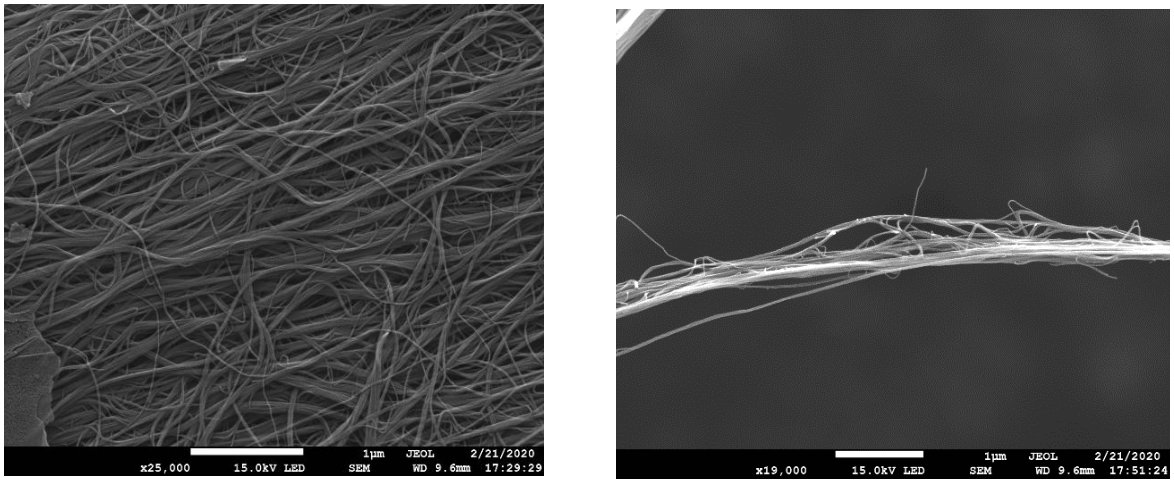

(a) (b)

Figure 8. SEM images exhibiting the morphology of 30 MWCNT sheets stacked on top of each other (a) and single MWCNT sheet (b).

Figure 8(a) shows the microstructural distribution of multi wall carbon nanotubes in our synthesized laminar composite structures. From this SEM image, it has been revealed that MWCNT bundles preferentially aligned in the direction of the sheet with interconnected structures but the multi wall carbon nanotubes become entangled each. Since the alignment and distribution of nanotubes have dominant effects on mechanical properties of structures, this entanglement of MWCNTs might have unfavorable effects on our synthesized yarn structure. Figure 8(b) represents the microscopic view of single MWCNT sheet which is used together to build up our laminar structure.

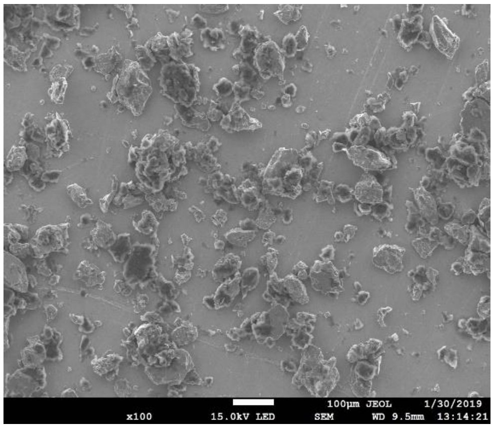

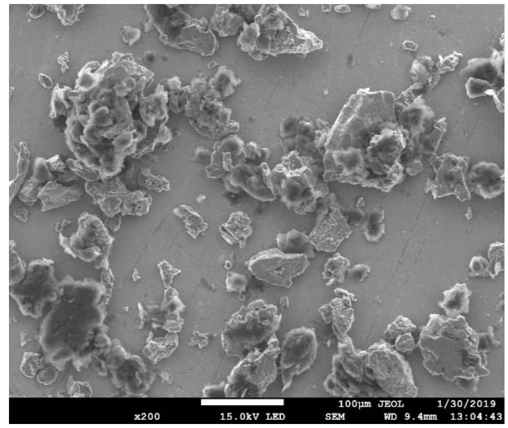

(a) (b)

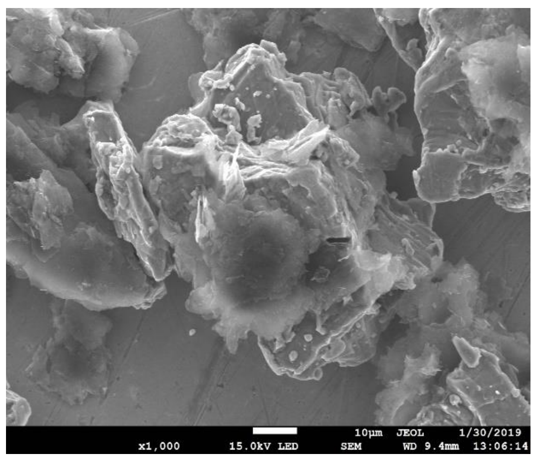

(c)

Figure 9. Microstructural distribution of synthesized TiC particles (a), (b) and deformations and fractures observed on TiC particle surface (c).

Figure 9, (a) and (b) reveal the microstructure examinations of synthesized TiC particles. The bright and dark regions in figure 9(a) and (b) are the TiC composites and unreacted Ti particles, respectively. One can assume that some titanium particles remain unreacted in titanium/graphene mixture due to lack of enough adsorbate (Graphene). This phenomenon also supports the XRD analysis of synthesized TiC particles. Shiny layers of TiC have been formed around the dark Ti particles. As well as it has been shown from the images that shape of the dark spots are irregular suggesting that Ti particle sizes are not uniform and average size is about 50-70 micrometer throughout the sample. Layered deformation and a series of fracturing steps were observed on particle surface in figure 9 (c). Irregular particle sizes and layered fracture on particles are expected in synthesized power because of using ball-miller to mix titanium/graphene together.

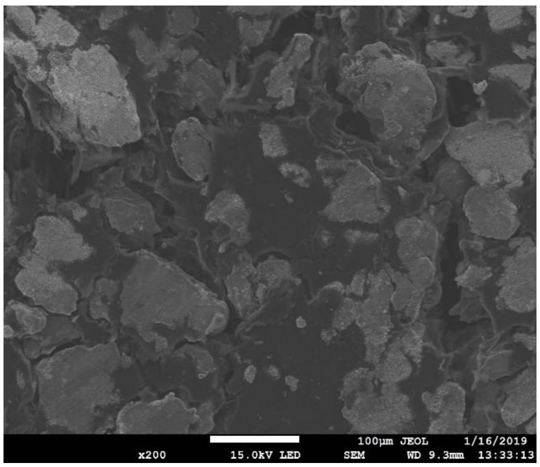

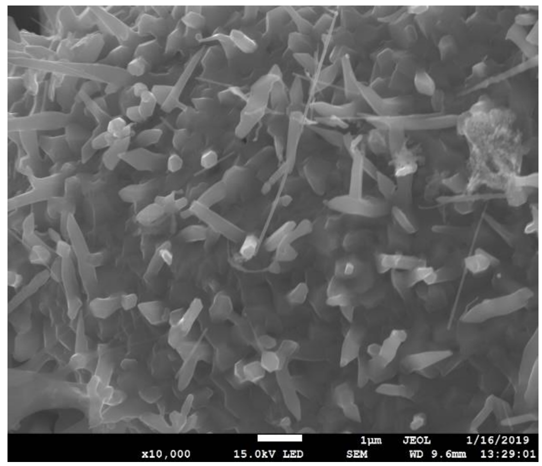

(a) (b)

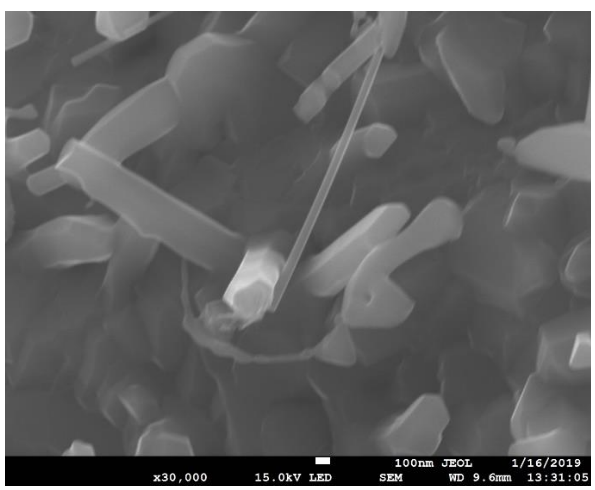

(c)

Figure 10. Representative SEM micrographs of synthesized TiC particles inside MWCNT laminar composite yarn (a), (b), and (c).

An evaluation of morphologies of in situ synthesized TiC particles inside MWCNT was shown in figure 10 (a), (b), and (c). It has been noticed from figure 10 (a) that produced TiC particles are nicely attached with MWCNT yarn. As well as sizes and shapes of particles are not uniform which is expected due to deformation and fracture occurred while using ball-miller to produce titanium/graphene mixture, and the dark flat surface represents the interior part of MWCNT yarn. Representative SEM morphology, figure 10 (b) and (c), reveals the nano scale distribution of TiC particles inside MWCNT yarn. Shiny particles inside MWCNT yarn are the synthesized TiC and tube-like bright lines are the nano carbon tubes in figure 10 (b). Nano sized TiC particle has been noticed (bright spot) inside MWCNT yarn in figure 10 (c).

4.4 Young's modulus analysis

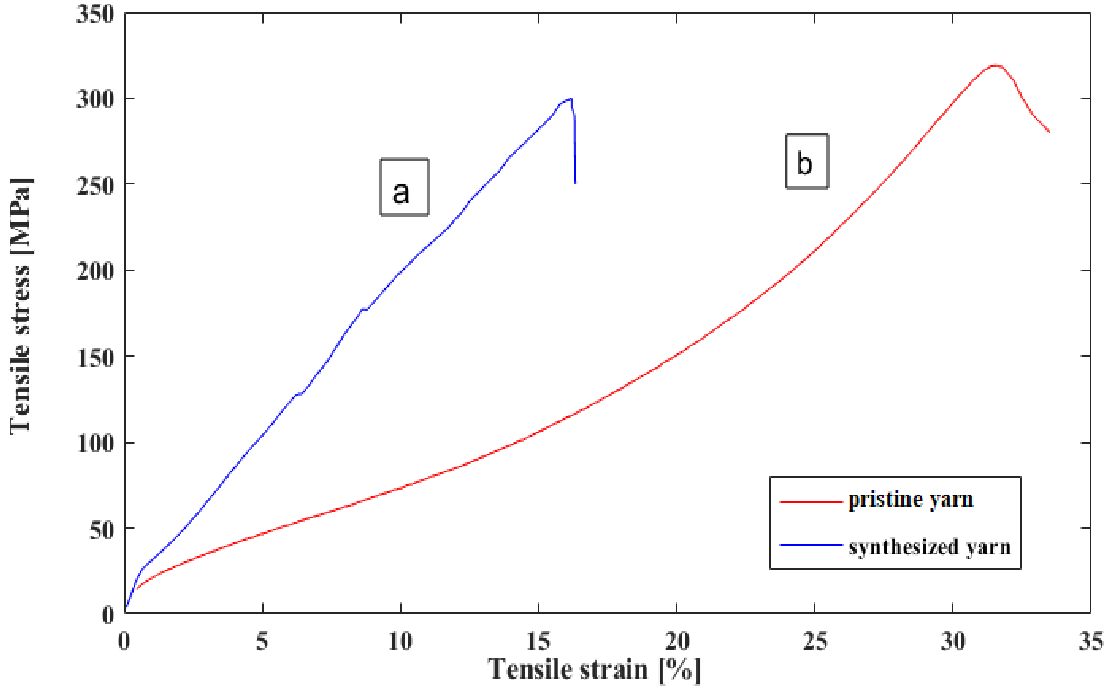

Figure 11. Tensile stress-strain curves for pristine MWCNT yarn and synthesized MWCNT yarn.

Figure 11. Blue curve (a) represents the stress-strain analysis for our synthesized laminar yarn reinforced with TiC and it has been shown that the increment of this curve is linear. The synthesized laminar composite structure exhibits excellent durability, with ultimate tensile strength value of 300 MPa for yarn reinforced with TiC, compared to a tensile strength value of 319 MPa for pristine MWCNT yarn (b). It can be concluded from figure 11 that synthesized yarn retains 70-80% of pristine MWCNT yarn strength.

Yarn types	Width (mm)	Thickness (mm)	Gauge length (mm)	Max. Load (N)	Stress (MPa)	Strain (mm/ mm)	Young's Modulus E (GPa)
Pristine (MWCNT)	0.06	0.06	7.50	2.34	319	0.32	1.00
Synthesized (Reinforced)	0.13	0.13	7.50	3.29	300	0.16	1.90

Table 2. Stress, Strain and Young's modulus values of pristine and synthesized yarn.

Young's modulus calculation for our synthesized yarn reinforced with TiC:

$$Young's\ modulus, E = \frac{stress}{strain}\ Pa$$

$$= \frac{300}{0.16}\ MPa$$

$$= 1.9\ GPa$$

Young's modulus calculation for pristine yarn:

$$Young's\ modulus, E = \frac{stress}{strain}\ Pa$$

$$= \frac{319}{0.32}\ MPa$$

$$= 1\ GPa$$

$$Percent\ increase\ of\ Young's\ modulus, E = \frac{1.9-1}{1} .100\%$$

$$= 90\ \%$$

Table 2 shows the tensile strength and young's modulus values for our synthesized and pristine yarn. From this above calculation, it has been shown that Young's Modulus of 1.9 GPa for reinforced yarn which is 90% greater than that the young's modulus of 1 GPa for pristine yarn.

CHAPTER V

CONCLUSIONS

In conclusions, we would like to summarize the main points of this work with some remarks on the results. This whole study has been accomplished into two different sections.

In the first section, it can be concluded from DSC and XRD analysis that TiC have been successfully investigated from titanium and graphene mixture at their stochiometric ratio. Even though some unreacted Ti particles were left in Ti/Gr mixture, nearly full conversion of mixture gets into TiC in XRD level. We can assume the probable reasons for these remaining unreacted particles due to high concentration of Ti present in Ti/Graphene mixture. As well as the shape and sizes of TiC has been recognized from the SEM particles morphologies.

In the second section, reinforcement of MWCNT laminar composite structure or yarn has been successful by in situ formation of TiC, which can be confirmed from the DSC analysis and composite morphologies investigated by using the thermal field emission Scanning Electron Microscope (SEM, JOEL).

The as-produced laminar composite structure exhibits excellent durability, with ultimate tensile strength value of 300 MPa for yarn reinforced with TiC, compared to a tensile strength value of 319 MPa for pristine MWCNT yarn. That means synthesized yarn can retain 90-95 % of strength of pristine MWCNT yarn which is really fascinating for the structural applications. Moreover, synthesized yarn shows the young's modulus of 1.9 GPa which is 90 % greater than that the young's modulus of 1 GPa for pristine MWCNT yarn.

We assume that tensile strength of our reinforced laminar composite structure or yarn can be improved more if you could overcome the following limitations what we have already faced during the experiments:

1) MWCNT alignment in the synthesized yarn is very crucial factor to improve the mechanical properties. Maintaining perfect alignment while making MWCNT yarn by hand is difficult, instead you could use automatic motor to produce perfect aligned MWCNT sheets stacked on top of each other.
2) Maintaining homogeneous dispersion of sample powder inside MWCNT sheets is also challenging. This inhomogeneous dispersion may restrain the load transfer inside MWCNT yarn.
3) We could use smaller Ti particles to mix with graphene nanoflakes.

REFERENCES

1. Jiang, Q., Wang, X., Zhu, Y., Hui, D., & Qiu, Y. (2014). Mechanical, electrical and thermal properties of aligned carbon nanotube/polyimide composites. *Composites Part B: Engineering*, *56*, 408-412.

2. Singh, V., Joung, D., Zhai, L., Das, S., Khondaker, S. I., & Seal, S. (2011). Graphene based materials: past, present and future. *Progress in materials science*, *56*(8), 1178-1271.

3. Moghadam, A. D., Omrani, E., Menezes, P. L., & Rohatgi, P. K. (2015). Mechanical and tribological properties of self-lubricating metal matrix nanocomposites reinforced by carbon nanotubes (CNTs) and graphene–a review. *Composites Part B: Engineering*, *77*, 402-420.

4. Zhai, W., Shi, X., Yao, J., Ibrahim, A. M. M., Xu, Z., Zhu, Q., ... & Zhang, Q. (2015). Investigation of mechanical and tribological behaviors of multilayer graphene reinforced Ni3Al matrix composites. *Composites Part B: Engineering*, *70*, 149-155.

5. Choi, B. K., Yoon, G. H., & Lee, S. (2016). Molecular dynamics studies of CNT-reinforced aluminum composites under uniaxial tensile loading. *Composites Part B: Engineering*, *91*, 119-12

6. Tong, L., Sun, X., & Tan, P. (2008). Effect of long multi-walled carbon nanotubes on delamination toughness of laminated composites. *Journal of Composite Materials*, *42*(1), 5-23.

7. Sugano, K., Kurata, M., & Kawada, H. (2014). Evaluation of mechanical properties of untwisted carbon nanotube yarn for application to composite materials. *Carbon*, *78*, 356-365.

8. Shin, S. E., Ko, Y. J., & Bae, D. (2016). Mechanical and thermal properties of nanocarbon-reinforced aluminum matrix composites at elevated temperatures. *Composites Part B: Engineering*, *106*, 66-73.

9. Li, Y., Wang, S., & Wang, Q. (2017). Enhancement of tribological properties of polymer composites reinforced by functionalized graphene. *Composites Part B: Engineering*, *120*, 83-91.

10. Fritscher, K., Peters, M., & Ratzer-Scheibe, H. J. (1992). Advanced Aerospace Materials, edited by H. Buhl.

11. Ebbesen, T. W. (1996). *Carbon nanotubes: preparation and properties*. CRC press.

12. Ismail, A. F., Goh, P. S., Sanip, S. M., & Aziz, M. (2009). Transport and separation properties of carbon nanotube-mixed matrix membrane. *Separation and Purification Technology*, *70*(1), 12-26.

13. Alvarez, N. T., Ruff, B., Haase, M., Malik, R., Kienzle, N., Mast, D., ... & Shanov, V. (2013). Carbon nanotube fiber spinning, densification, doping and coating for microcable manufacturing. *WSEAS Proc.: Recent Adv. in Circuits, Communications and Signal Proc*, 336-41.

14. Tran, C. D., Humphries, W., Smith, S. M., Huynh, C., & Lucas, S. (2009). Improving the tensile strength of carbon nanotube spun yarns using a modified spinning process. *Carbon*, *47*(11), 2662-2670.

15. Afolabi, A. S., Abdulkareem, A. S., Iyuke, S. E., & van Zyl Pienaar, H. C. (2009). Continuous production of carbon nanotubes and diamond films by swirled floating catalyst chemical vapour deposition method. *South African Journal of Science*, *105*(7-8), 278-281.

16. Hobosyan, M. A., Martinez, P. M., Zakhidov, A. A., Haines, C. S., Baughman, R. H., & Martirosyan, K. S. (2017). Laminar composite structures for high power actuators. *Applied Physics Letters*, *110*(20), 203101.

17. Zhang, X., Jiang, K., Feng, C., Liu, P., Zhang, L., Kong, J., ... & Fan, S. (2006). Spinning and processing continuous yarns from 4-inch wafer scale super-aligned carbon nanotube arrays. *Advanced materials*, *18*(12), 1505-1510.

18. Vilatela, J. J., & Windle, A. H. (2012). A multifunctional yarn made of carbon nanotubes. *Journal of Engineered Fibers and Fabrics*, *7*(2_suppl), 155892501200702S04.

19. Zhang, M., Atkinson, K. R., & Baughman, R. H. (2004). Multifunctional carbon nanotube yarns by downsizing an ancient technology. *Science*, *306*(5700), 1358-1361.

20. Qu, L., Dai, L., Stone, M., Xia, Z., & Wang, Z. L. (2008). Carbon nanotube arrays with strong shear binding-on and easy normal lifting-off. *Science*, *322*(5899), 238-242.

21. Xu, M., Futaba, D. N., Yamada, T., Yumura, M., & Hata, K. (2010). Carbon nanotubes with temperature-invariant viscoelasticity from–196 to 1000 C. *Science*, *330*(6009), 1364-1368.

22. Aliev, A. E., Oh, J., Kozlov, M. E., Kuznetsov, A. A., Fang, S., Fonseca, A. F., ... & Zhang, M. (2009). Giant-stroke, superelastic carbon nanotube aerogel muscles. *science*, *323*(5921), 1575-1578.

23. Geim, A. K. (2009). Graphene: status and prospects. *science*, *324*(5934), 1530-1534.

24. Nieto, A., Bisht, A., Lahiri, D., Zhang, C., & Agarwal, A. (2017). Graphene reinforced metal and ceramic matrix composites: a review. *International Materials Reviews*, *62*(5), 241-302.

25. Mohan, V. B., Lau, K. T., Hui, D., & Bhattacharyya, D. (2018). Graphene-based materials and their composites: a review on production, applications and product limitations. *Composites Part B: Engineering*, *142*, 200-220.

26. Stoller, M. D., Park, S., Zhu, Y., An, J., & Ruoff, R. S. (2008). Graphene-based ultracapacitors. *Nano letters*, *8*(10), 3498-3502.

27. Robinson, J. T., Perkins, F. K., Snow, E. S., Wei, Z., & Sheehan, P. E. (2008). Reduced graphene oxide molecular sensors. *Nano letters*, *8*(10), 3137-3140.

28. Tung, V. C., Chen, L. M., Allen, M. J., Wassei, J. K., Nelson, K., Kaner, R. B., & Yang, Y. (2009). Low-temperature solution processing of graphene− carbon nanotube hybrid materials for high-performance transparent conductors. *Nano letters*, *9*(5), 1949-1955.

29. Wang, D. W., Li, F., Zhao, J., Ren, W., Chen, Z. G., Tan, J., ... & Cheng, H. M. (2009). Fabrication of graphene/polyaniline composite paper via in situ anodic electropolymerization for high-performance flexible electrode. *ACS nano*, *3*(7), 1745-1752.

30. Li, X., Wang, X., Zhang, L., Lee, S., & Dai, H. (2008). Chemically derived, ultrasmooth graphene nanoribbon semiconductors. *science*, *319*(5867), 1229-1232.

31. Balandin, A. A., Ghosh, S., Bao, W., Calizo, I., Teweldebrhan, D., Miao, F., & Lau, C. N. (2008). Superior thermal conductivity of single-layer graphene. *Nano letters*, *8*(3), 902-907

32. Hu, Z., Tong, G., Nian, Q., Xu, R., Saei, M., Chen, F., ... & Xu, J. (2016). Laser sintered single layer graphene oxide reinforced titanium matrix nanocomposites. *Composites Part B: Engineering*, *93*, 352-359.

33. Seagle, S. R. (2000). Titanium and titanium alloys. *Kirk-Othmer Encyclopedia of Chemical Technology*

34. Kondoh, K., Threrujirapapong, T., Imai, H., Umeda, J., & Fugetsu, B. (2009). Characteristics of powder metallurgy pure titanium matrix composite reinforced with multi-wall carbon nanotubes. *Composites Science and Technology*, *69*(7-8), 1077-1081.

35. Melendez, I. M., Neubauer, E., Angerer, P., Danninger, H., & Torralba, J. M. (2011). Influence of nano-reinforcements on the mechanical properties and microstructure of titanium matrix composites. *Composites Science and Technology*, *71*(8), 1154-1162.

36. Hu, Z., Chen, F., Xu, J., Ma, Z., Guo, H., Chen, C., ... & Zhang, M. (2018). Fabricating graphene-titanium composites by laser sintering PVA bonding graphene titanium coating: Microstructure and mechanical properties. *Composites Part B: Engineering*, *134*, 133-140.

37. Zhang, Y. H., Yue, L. J., Han, L. F., Chen, J. L., Jia, D. Z., & Li, F. (2012). Tuning the magnetic and transport property of graphene with Ti atom and cluster. *Computational Materials Science*, *56*, 95-99.

38. Kaushik, V., Shukla, A. K., & Vankar, V. D. (2013). Improved electron field emission from metal grafted graphene composites. *Carbon*, *62*, 337-345.

39. Yao, Z., Stiglich, J. J., & Sudarshan, T. S. (1999). Nano-grained tungsten carbide–cobalt (WC/Co). *Mater. Modif*, 1-27.

40. Galevsky, G. V., Rudneva, V. V., Garbuzova, A. K., & Valuev, D. V. (2015). Titanium carbide: nanotechnology, properties, application. In *IOP Conference Series: Materials Science and Engineering* (Vol. 91, No. 1, p. 012017). IOP Publishing.

41. Liang, Y., & Dutta, S. P. (2001). Application trend in advanced ceramic technologies. *Technovation*, *21*(1), 61-65.

42. Pierson, H. O. (1999). *Handbook of chemical vapor deposition: principles, technology and applications*. William Andrew.

43. Srivastava, A. K., & Das, K. (2009). Microstructural and mechanical characterization of in situ TiC and (Ti, W) C-reinforced high manganese austenitic steel matrix composites. *Materials Science and Engineering: A*, *516*(1-2), 1-6.

44. Zhong, L., Xu, Y., Hojamberdiev, M., Wang, J., & Wang, J. (2011). In situ fabrication of titanium carbide particulates-reinforced iron matrix composites. *Materials & design*, *32*(7), 3790-3795.

45. Sun, G. J., Wu, S. J., & Su, G. C. (2010). Research on impact wear resistance of in situ reaction TiCp/Fe composite. *Wear*, *269*(3-4), 285-290.

46. Akhtar, F., & Guo, S. J. (2008). Microstructure, mechanical and fretting wear properties of TiC-stainless steel composites. *Materials Characterization*, *59*(1), 84-90.

47. HACK, C. (1987). Dispersion strengthened alloys for aerospace. *Metals and materials*, *3*(8), 457-462.

48. Froes, F. H., & DeBarbadillo, J. J. (1990). *Structural applications of mechanical alloying: proceedings of an ASM International conference, Myrtle Beach, South Carolina, 27-29 March 1990*. Asm Intl.

49. Chu, K., Jia, C. C., Li, W. S., & Wang, P. (2013). Mechanical and electrical properties of carbon-nanotube-reinforced Cu–Ti alloy matrix composites. *physica status solidi (a)*, *210*(3), 594-599.

50. He, C. N., Zhao, N. Q., Shi, C. S., & Song, S. Z. (2009). Mechanical properties and microstructures of carbon nanotube-reinforced Al matrix composite fabricated by in situ chemical vapor deposition. *Journal of Alloys and Compounds*, *487*(1-2), 258-262.

51. Kondoh, K., Fukuda, H., Umeda, J., Imai, H., Fugetsu, B., & Endo, M. (2010). Microstructural and mechanical analysis of carbon nanotube reinforced magnesium alloy powder composites. *Materials Science and Engineering: A*, *527*(16-17), 4103-4108.

52. Sadeghi, N., Aghajani, H., & Akbarpour, M. R. (2018). Microstructure and tribological properties of in-situ TiC-C/Cu nanocomposites synthesized using different carbon sources (graphite, carbon nanotube and graphene) in the Cu-Ti-C system. *Ceramics International*, *44*(18), 22059-22067.

53. Yang, Q., Senda, T., & Ohmori, A. (2003). Effect of carbide grain size on microstructure and sliding wear behavior of HVOF-sprayed WC–12% Co coatings. *Wear*, *254*(1-2), 23-34.

54. Popov, V. A., Shelekhov, E. V., Prosviryakov, A. S., Presniakov, M. Y., Senatulin, B. R., Kotov, A. D., & Khomutov, M. G. (2017). Particulate metal matrix composites

development on the basis of in situ synthesis of TiC reinforcing nanoparticles during mechanical alloying. *Journal of Alloys and Compounds*, *707*, 365-370.

55. He, B., Chang, K., Wu, W., & Zhang, C. (2017). The formation mechanism of TiC reinforcement and improved tensile strength in additive manufactured Ti matrix nanocomposite. *Vacuum*, *143*, 23-27.

56. Yin, X., Gotman, I., Klinger, L., & Gutmanas, E. Y. (2005). Formation of titanium carbide on graphite via powder immersion reaction assisted coating. *Materials Science and Engineering: A*, *396*(1-2), 107-114

57. Tong, L., & Reddy, R. G. (2005). Synthesis of titanium carbide nano-powders by thermal plasma. *Scripta Materialia*, *52*(12), 1253-1258

58. Swift, G. A., & Koc, R. (1999). Formation studies of TiC from carbon coated TiO2. *Journal of materials science*, *34*(13), 3083-3093

59. Tjong, S. C., & Ma, Z. Y. (2000). Microstructural and mechanical characteristics of in situ metal matrix composites. *Materials Science and Engineering: R: Reports*, *29*(3-4), 49-113.

60. Zohari, S., Sadeghian, Z., Lotfi, B., & Broeckmann, C. (2015). Application of spark plasma sintering (SPS) for the fabrication of in situ Ni–TiC nanocomposite clad layer. *Journal of Alloys and Compounds*, *633*, 479-483.

61. ASHITANI, T., TOMOSHIGE, R., OYADOMARI, M., UENO, T., & SAKAI, K. (2002). Synthesis of titanium carbide from woody materials by self-propagating high temperature synthesis. *Journal of the Ceramic Society of Japan*, *110*(1283), 632-638.

62. Nersisyan, H. H., Lee, J. H., & Won, C. W. (2003). Combustion of TiO2–Mg and TiO2–Mg–C systems in the presence of NaCl to synthesize nanocrystalline Ti and TiC powders. *Materials research bulletin*, *38*(7), 1135-1146.

63. Licheri, R., Orrù, R., & Cao, G. (2004). Chemically-activated combustion synthesis of TiC–Ti composites. *Materials Science and Engineering: A*, *367*(1-2), 185-197

64. Ye, L. L., & Quan, M. X. (1995). Synthesis of nanocrystalline TiC powders by mechanical alloying. *Nanostructured materials*, *5*(1), 25-31

65. Yang, W. Z., Huang, W. M., Wang, Z. F., Shang, F. J., Huang, W., & Zhang, B. Y. (2016). Thermal and mechanical properties of graphene–titanium composites synthesized by microwave sintering. *Acta Metallurgica Sinica (English Letters)*, *29*(8), 707-713.

66. Manukyan, K. V., Lin, Y. C., Rouvimov, S., McGinn, P. J., & Mukasyan, A. S. (2013). Microstructure-reactivity relationship of Ti+ C reactive nanomaterials. *Journal of Applied Physics*, *113*(2), 024302.

67. Tjong, S. C., & Ma, Z. Y. (2000). Microstructural and mechanical characteristics of in situ metal matrix composites. *Materials Science and Engineering: R: Reports*, *29*(3-4), 49-113.

68. Huang, X., Yin, C., Zhao, Z., Zhang, L., & Wu, J. (2015). Microstructures and Toughening of TiC-TiB2 Ceramic Composites with Cr-Based Alloy Phase Prepared by Combustion Synthesis in High-Gravity Field. *Advances in Materials Science and Engineering*, *2015*.

69. Nersesyan, M. D., Avakyan, P. B., Martirosyan, K. S., Komarov, A. V., & Merzhanov, A. G. (1993). Self-propagating high-temperature synthesis of ferrites. *Inorg. Mater.*, *29*(12), 1506-1508.

70. Tolendiuly, S., Fomenko, S. M., Dannangoda, G. C., & Martirosyan, K. S. (2017). Self-Propagating High Temperature Synthesis of MgB2 Superconductor in High-Pressure of Argon Condition. *Eurasian Chemico-Technological Journal*, *19*(2), 177-181.

71. Martirosyan, K. S., Galstyan, E., Hossain, S. M., Wang, Y. J., & Litvinov, D. (2011). Barium hexaferrite nanoparticles: synthesis and magnetic properties. *Materials Science and Engineering: B*, *176*(1), 8-13.

72. Martirosyan, K. S., & Luss, D. (2007). Carbon combustion synthesis of ferrites: synthesis and characterization. *Industrial & engineering chemistry research*, *46*(5), 1492-1499.

73. Saukhimov, A. A., Hobosyan, M. A., Dannangoda, G. C., Zhumabekova, N. N., Almanov, G. A., Kumekov, S. E., & Martirosyan, K. S. (2015). Solution-combustion synthesis and magnetodielectric properties of nanostructured rare earth ferrites. *International Journal of Self-Propagating High-Temperature Synthesis*, *24*(2), 63-71

74. Mamyrbaeva, Y., Hobosyan, M. A., Kumekov, S. E., & Martirosyan, K. S. (2013). Carbon combustion synthesis of lithium cobaltate. *NSTI-Nano-Tech*, *2*, 657-659.

75. KS. Martirosyan, C. Dannangoda, E. Galstyan, and D. Litvinov, Screen-printing of ferrite magnetic nanoparticles produced by carbon combustion synthesis of oxides, J. Appl. Phys., 111, 094311, 2012.

76. M. A. Hobosyan and K. S. Martirosyan, Consolidation of Lunar Regolith Simulant by Activated Thermite Reactions, J. Aerosp. Eng., 04014105-1- 04014105-9, 2014.

77. M.K. Atamanov, I. Noboru, T. Shotaro, R. Amrousse, M.Y. Tulepov, A.R. Kerimkulova, M.A. Hobosyan, K. Hori, K.S. Martirosyan, Z.A. Mansurov, Investigation of Combustion and Thermal Analysis of Ammonium Nitrate with Carbonaceous Materials, Combustion Science and Technology, 188 (11-12), 2003-2011, 2016.

78. A.A. Markov, M.A. Hobosyan, and K.S. Martirosyan, Slip-Jump Model for Carbon Combustion Synthesis of Complex Oxide Nanoparticles, Eurasian Chemico-Technological Journal 18, 223-233, 2016.

79. A.A. Markov, I.A. Filimonov, and K.S. Martirosyan, Modeling of Submicron Complex Oxides Synthesis, Theoretical Foundations of Chemical Engineering, 51, 1, 27–37. 2017.

80. A. Markov, I. Filimonov, and K.S. Martirosyan, Complex Effect of Mach, Peclet and Reynolds Numbers on the CCSO Gas Dynamics Features, Int. J. of SHS, 22, 11-17, 2013.

81. A. Markov, I. Filimonov, and K.S. Martirosyan, Simulation of front motion in a reacting condensed two phase mixture, J. of Computational Physics, 231, 6714–6724, 2012.

82. K.S. Martirosyan, and A.S. Mukasyan, "Combustion Synthesis of Nanomaterials", In Dekker Encyclopedia of Nanoscience and Nanotechnology, Third Edition. CRC Press: New York, 983–1001, 2014

83. Eslamloo-Grami, M., & Munir, Z. A. (1990). Effect of nitrogen pressure and diluent content on the combustion synthesis of titanium nitride. *Journal of the American Ceramic Society*, *73*(8), 2222-2227.

84. Hoke, D. A., & Meyers, M. A. (1995). Consolidation of Combustion-Synthesized Titanium Diboride-Based Materials. *Journal of the American Ceramic Society*, *78*(2), 275-284.

85. Philpot, K. A., Munir, Z. A., & Holt, J. B. (1987). An investigation of the synthesis of nickel aluminides through gasless combustion. *Journal of materials science*, *22*(1), 159-169.

86. Hernandez-Guerrero, A., Huque, Z., & Kanury, A. M. (1992). An experimental investigation of combustive synthesis of titanium carbide. *Combustion science and technology*, *81*(1-3), 115-128.

87. Moore, J. J., & Feng, H. J. (1995). Combustion synthesis of advanced materials: Part II. Classification, applications and modelling. *Progress in Materials Science*, *39*(4-5), 275-316.

88. Bowen, C. R., & Derby, B. (1997). Selfpropagating high temperature synthesis of ceramic materials. *British ceramic transactions*, *96*(1), 25-31.

89. Holt, J. B., & Munir, Z. A. (1986). Combustion synthesis of titanium carbide: theory and experiment. *Journal of Materials Science*, *21*(1), 251-259.

90. Yamada, O., Miyamoto, Y., & Koizumi, M. (1987). High-Pressure Self-Combustion Sintering of Titanium Carbide. *Journal of the American Ceramic Society*, *70*(9), C-206.

91. Thiagarajan, V., Wang, X., Bradford, P. D., Zhu, Y. T., & Yuan, F. G. (2014). Stabilizing carbon nanotube yarns using chemical vapor infiltration. *Composites science and technology*, *90*, 82-87.

92. Bogdanovich, A. E., & Bradford, P. D. (2010). Carbon nanotube yarn and 3-D braid composites. Part I: Tensile testing and mechanical properties analysis. *Composites Part A: Applied Science and Manufacturing*, *41*(2), 230-237.

93. Olek, M., Ostrander, J., Jurga, S., Möhwald, H., Kotov, N., Kempa, K., & Giersig, M. (2004). Layer-by-layer assembled composites from multiwall carbon nanotubes with different morphologies. *Nano letters*, *4*(10), 1889-1895.

94. Wang, X., Bradford, P. D., Liu, W., Zhao, H., Inoue, Y., Maria, J. P., ... & Zhu, Y. (2011). Mechanical and electrical property improvement in CNT/Nylon composites through drawing and stretching. *Composites Science and Technology*, *71*(14), 1677-1683.

95. Jayasinghe, C., Amstutz, T., Schulz, M. J., & Shanov, V. (2013). Improved processing of carbon nanotube yarn. *Journal of Nanomaterials*, *2013*.

96. Zhang, M., Atkinson, K. R., & Baughman, R. H. (2004). Multifunctional carbon nanotube yarns by downsizing an ancient technology. *Science*, *306*(5700), 1358-1361.

97. Zhu, H. W., Xu, C. L., Wu, D. H., Wei, B. Q., Vajtai, R., & Ajayan, P. M. (2002). Direct synthesis of long single-walled carbon nanotube strands. *Science*, *296*(5569), 884-886.

98. Miller, S. G., Williams, T. S., Baker, J. S., Solá, F., Lebron-Colon, M., McCorkle, L. S., ... & Meador, M. A. (2014). Increased tensile strength of carbon nanotube yarns and

sheets through chemical modification and electron beam irradiation. *ACS applied materials & interfaces*, *6*(9), 6120-6126.

99. Liu, K., Sun, Y., Lin, X., Zhou, R., Wang, J., Fan, S., & Jiang, K. (2010). Scratch-resistant, highly conductive, and high-strength carbon nanotube-based composite yarns. *ACS nano*, *4*(10), 5827-5834.

100. Tanner, K. E. (2002). Titanium in medicine. *Proceedings of the Institution of Mechanical Engineers, Part H: Journal of Engineering in Medicine*, *216*(3), 215-215.

101. Textor, M., Sittig, C., Frauchiger, V., Tosatti, S., & Brunette, D. M. (2001). Properties and biological significance of natural oxide films on titanium and its alloys. In *Titanium in medicine* (pp. 171-230). Springer, Berlin, Heidelberg.

102. Mauter, M. S., & Elimelech, M. (2008). Environmental applications of carbon-based nanomaterials. *Environmental Science & Technology*, *42*(16), 5843-5859.

103. Karami, M., Bahabadi, M. A., Delfani, S., & Ghozatloo, A. (2014). A new application of carbon nanotubes nanofluid as working fluid of low-temperature direct absorption solar collector. *Solar Energy Materials and Solar Cells*, *121*, 114-118.

104. Robertson, D. H., Brenner, D. W., & Mintmire, J. W. (1992). Energetics of nanoscale graphitic tubules. *Physical Review B*, *45*(21), 12592.

105. Yu, M. F., Files, B. S., Arepalli, S., & Ruoff, R. S. (2000). Tensile loading of ropes of single wall carbon nanotubes and their mechanical properties. *Physical review letters*, *84*(24), 5552.

106. Saifuddin, N., Raziah, A. Z., & Junizah, A. R. (2012). Carbon nanotubes: a review on structure and their interaction with proteins. *Journal of Chemistry*, *2013*.

107. Ma, L., Hendrickson, K. E., Wei, S., & Archer, L. A. (2015). Nanomaterials: Science and applications in the lithium–sulfur battery. *Nano Today*, *10*(3), 315-338.

108. Shende, R. C., & Ramaprabhu, S. (2016). Thermo-optical properties of partially unzipped multiwalled carbon nanotubes dispersed nanofluids for direct absorption solar thermal energy systems. *Solar Energy Materials and Solar Cells*, *157*, 117-125.

109. Li, X., Zou, C., Chen, W., & Lei, X. (2016). Experimental investigation of β-cyclodextrin modified carbon nanotubes nanofluids for solar energy systems: Stability, optical properties and thermal conductivity. *Solar Energy Materials and Solar Cells*, *157*, 572-579.

110. Dürkop, T., Getty, S. A., Cobas, E., & Fuhrer, M. S. (2004). Extraordinary mobility in semiconducting carbon nanotubes. *Nano letters*, *4*(1), 35-39.

111. Wang, F., Kozawa, D., Miyauchi, Y., Hiraoka, K., Mouri, S., Ohno, Y., & Matsuda, K. (2015). Considerably improved photovoltaic performance of carbon nanotube-based solar cells using metal oxide layers. *Nature communications*, *6*(1), 1-7.

112. Sharma, P., & Ahuja, P. (2008). Recent advances in carbon nanotube-based electronics. *Materials Research Bulletin*, *43*(10), 2517-2526.

113. Wang, W., & Kumta, P. N. (2010). Nanostructured hybrid silicon/carbon nanotube heterostructures: reversible high-capacity lithium-ion anodes. *ACS nano*, *4*(4), 2233-2241.

114. Wu, H., Chan, G., Choi, J. W., Ryu, I., Yao, Y., McDowell, M. T., ... & Cui, Y. (2012). Stable cycling of double-walled silicon nanotube battery anodes through solid–electrolyte interphase control. *Nature nanotechnology*, *7*(5), 310.

115. Pokhrel, L. R., Ettore, N., Jacobs, Z. L., Zarr, A., Weir, M. H., Scheuerman, P. R., ... & Dubey, B. (2017). Novel carbon nanotube (CNT)-based ultrasensitive sensors for trace mercury (II) detection in water: A review. *Science of the Total Environment*, *574*, 1379-1388.

116. Qiu, W., Xu, H., Takalkar, S., Gurung, A. S., Liu, B., Zheng, Y., ... & Liu, G. (2015). Carbon nanotube-based lateral flow biosensor for sensitive and rapid detection of DNA sequence. *Biosensors and Bioelectronics*, *64*, 367-372.

117. Novoselov, K. S., Geim, A. K., Morozov, S. V., Jiang, D., Zhang, Y., Dubonos, S. V., & Firsov, A. A. (2004). Electric field effect in atomically thin carbon films. *science*, *306*(5696), 666-669.

BIOGRAPHICAL SKETCH

Rakibul Alam Shohan was born on 6th July, 1989 in Bhaluka, Mymensingh, Bangladesh. He earned his Bachelor of Science degree in physics and Master of Science degree in physics (Condensed matter physics) from the University of Dhaka, Bangladesh in 2013 and 2015, respectively. In 2020, he received his second Master of Science degree in physics (Nano Science and Material Science) from the University of Texas Rio Grande Valley. He is going to pursue his Doctor of Philosophy in physics at The University of Texas at San Antonio. He personal email address is shohanshikder.phdu@gmail.com.